Published in final edited form as:
Cancer Res. 2014 December 15; 74(24): 7217–7228. doi:10.1158/0008-5472.CAN-14-0505.

Adaptive Responses to Dasatinib-Treated Lung Squamous Cell Cancer Cells Harboring DDR2 Mutations

Yun Bai[#1], **Jae-Young Kim**[#1], **January M. Watters**[2], **Bin Fang**[3], **Fumi Kinose**[1], **Lanxi Song**[1], **John M. Koomen**[4], **Jamie K. Teer**[5], **Kate Fisher**[5], **Yian Ann Chen**[5], **Uwe Rix**[2], and **Eric B. Haura**[1,*]

[1]Department of Thoracic Oncology, H. Lee Moffitt Cancer Center and Research Institute, Tampa, FL 33612

[2]Department of Drug Discovery, H. Lee Moffitt Cancer Center and Research Institute, Tampa, FL 33612

[3]Proteomics Core Facility, H. Lee Moffitt Cancer Center and Research Institute, Tampa, FL 33612

[4]Department of Molecular Oncology, H. Lee Moffitt Cancer Center and Research Institute, Tampa, FL 33612

[5]Department of Biostatistics and Bioinformatics, H. Lee Moffitt Cancer Center and Research Institute, Tampa, FL 33612

[#] These authors contributed equally to this work.

Abstract

DDR2 mutations occur in ~4% of lung squamous cell cancer (SCC) where the tyrosine kinase inhibitor dasatinib has emerged as a new therapeutic option. We found that ERK and AKT phosphorylation was weakly inhibited by dasatinib in DDR2-mutant lung SCC cells, suggesting that dasatinib inhibits survival signals distinct from other oncogenic RTKs and/or compensatory signals exist that dampen dasatinib activity. To gain better insight into dasatinib's action in these cells, we assessed altered global tyrosine phosphorylation (pY) after dasatinib exposure, employing a mass spectrometry (MS)-based quantitative phosphoproteomics approach. Overlaying protein-protein interaction relationships upon this dasatinib-regulated pY network revealed decreased phosphorylation of Src family kinases and their targets. Conversely, dasatinib enhanced tyrosine phosphorylation in a panel of receptor tyrosine kinases (RTK) and their signaling adaptor complexes, including EGFR, MET/GAB1, and IGF-1R/IRS2, implicating a RTK-driven adaptive response associated with dasatinib. To address the significance of this observation, these results were further integrated with results from a small molecule chemical library screen. We found that dasatinib combined with MET and IGF-1R inhibitors had a

[*]Corresponding Author: Eric B Haura, MD, Department of Thoracic Oncology, Chemical Biology and Molecular Medicine Program, H. Lee Moffitt Cancer Center and Research Institute, MRC3East, Room 3056F, 12902 Magnolia Drive, Tampa, Florida 33612 (Phone: 813-903-6827; Fax: 813-903-6817; eric.haura@moffitt.org)..

Conflict of interest statement: E.B. Haura received research funding from Bristol Myers Oncology to support a clinical study examining dasatinib for the treatment of DDR2 mutant lung cancer. No potential conflicts of interest were disclosed by the other authors.

synergistic effect and ligand stimulation of EGFR and MET rescued DDR2-mutant lung SCC cells from dasatinib-induced loss of cell viability. Importantly, we observed high levels of tyrosine-phosphorylated EGFR and MET in a panel of human lung SCC tissues harboring DDR2 mutations. Our results highlight potential RTK-driven adaptive resistant mechanisms upon DDR2 targeting, and they suggest new, rationale co-targeting strategies for DDR2-mutant lung SCC.

Keywords

DDR2; phosphoproteomics; squamous cell lung cancer; dasatinib; adaptive response

Introduction

Genetic alterations associated with the development of lung adenocarcinoma have been extensively characterized (1), and small molecule-based targeting of oncogenic kinases has resulted in great progress in this type of lung cancer (i.e., EGFR and ALK tyrosine kinase inhibitors) (2). However, driver mutations in lung squamous cell cancer (SCC), another major type of lung cancer, have been poorly characterized, and kinase inhibitors for lung adenocarcinoma have shown limited efficacy against lung SCC. Driver mutations responsible for lung SCC are increasingly being identified. FGFR1 amplification has been reported in lung SCC (22% frequency), which confers sensitivity to FGFR inhibitor (3), and copy number increases or mutations in PIK3CA have been found in lung SCC at 34.5% frequency (4). Recently, a comprehensive genomic approach has been conducted to delineate genetic alterations associated with lung SCC (5). Discoidin domain receptor 2 (DDR2) is one of the recently identified oncogenic driver kinases in lung SCC. DDR2 is a receptor tyrosine kinase (RTK) and a member of the DDR kinase family involved in cellular communication with extracellular matrix through binding of collagen (6). Recently, Hammerman and colleagues revealed a panel of DDR2 mutations in a fraction of lung SCC (approximately 4%), some of which induce oncogenic transformation (7). DDR2 mutations are associated with increased sensitivity to dasatinib, a multi-targeted tyrosine kinase inhibitor (TKI) inhibiting both non-RTKs (i.e., Src family kinase (SFK) members) and RTKs (i.e., ephrin receptors, DDR1 and DDR2) (7-11). The clinical activity of dasatinib in lung cancer is being evaluated in a number of clinical trials (12, 13). Of note, a recent case report provided further evidence of clinical activity of dasatinib in a patient with lung SCC harboring DDR2 mutation (14).

The nature of the DDR2 mutations and their role in downstream signaling in the context of SCC remain unclear. Original studies used classical transformation assays to show the oncogenic function of DDR2 mutations in fibroblast cells (7). Conversely, RNA interference studies and gatekeeper-mediated allele rescue supported DDR2 as the primary target of dasatinib in lung SCC harboring DDR2 mutations. More recent studies have suggested a tumor suppressor role of some DDR2 mutations in the context of collagen-directed signaling. The Huang lab showed reduced tyrosine phosphorylation of the I638F DDR2 mutation, and this was associated with reduced ability to suppress HEK293 growth in the presence of collagen (15). In our study, we characterized dasatinib's action on lung cancer signaling in lung SCC cell lines harboring activated mutations of DDR2 (7). Here, our study

focused on examining dasatinib-driven events in SCC cell lines harboring DDR2 mutations. This approach was designed to mimic clinical trials and decipher drug-induced mechanisms contributing to dasatinib's effects in these cells, rather than specifically to interrogate DDR2's function in lung cancer or to study the exact role of point mutations, which are still important to elucidate. We observed that dasatinib failed to completely abrogate phosphorylation of ERK, while it was completely reduced by other TKIs targeting EGFR and ALK in cancer cells harboring corresponding mutations. Employing a phosphotyrosine (pY) mass spectrometry analysis following dasatinib exposure, we show that dasatinib increased tyrosine phosphorylation of multiple RTKs, including EGFR, IGF-1R, MET, and ERBB2 (also called HER2), suggesting that increased RTK signaling compensates growth/survival signaling following dasatinib treatment in these DDR2-mutant cells. Chemical screening and ligand rescue experiments revealed rational co-targeting strategies as well as ligand-driven compensatory responses associated with dasatinib. Finally, we found a panel of DDR2-mutant human lung SCC tissues that exhibited intrinsically high levels of EGFR and MET, suggesting evidence of RTK-driven resistant mechanisms to dasatinib in DDR2-mutant human lung SCC.

Materials and Methods

A full description of all materials and methods can be found in the Supplementary Materials and Methods.

Cell lines

H2286 and HCC366 lung SCC cell lines, provided by Dr. Peter Hammerman (Dana-Farber Cancer Institute), were maintained in RPMI supplemented with 10% FBS. DDR2 mutations were genetically tested and authenticated using STR (Short Tandem Repeat; ACTG Inc) analysis. Cells were confirmed to be free of mycoplasma using PlasmoTest (InvivoGen).

Drugs

Dasatinib, cabozantinib, and crizotinib were purchased from ChemiTek. BMS-754807 and linsitinib were purchased from Active Biochem, lapatinib from LC Laboratories, and GSK183807A from SelleckChem. Ligands for RTKs were purchased from PeproTech.

Cell viability assay

Cell viability was analyzed by CellTiter-Glo (Promega) according to the manufacturer's recommendations. Cells, plated at 3×10^3 per well in black-wall 96-well plates, were exposed to drugs alone or in combination with RTK ligands the next day. Ninety-six hours (Fig. 1A) or 72 hours (Fig. 5 A and B) after treatment, 50 μL of CellTiter-Glo reagent were added and luminescence was recorded. The IC_{50} was defined as the drug concentration that induced 50% cell viability in comparison with DMSO control, which was calculated by non-linear regression analysis (Prism, GraphPad 5.0).

Cell cycle assay

Cells were fixed with ice-cold 70% ethanol in −20°C for overnight. The next day, cells were washed with PBS twice, treated with RNase A (325 μg/mL) at 37°C for 30 min, and then

stained with propidium iodide (50 μg/mL) at 4°C for 20 min. DNA contents were analyzed by flow cytometry.

Western blotting

Western blotting was performed as described in our previous studies (8, 16). Primary antibodies used for our study were purchased from Cell Signaling Technology except β-actin (Sigma-Aldrich). To quantify the intensity of the Western blot bands, MATLAB (2013b) software was employed. First, Western blot images were loaded by a command “imread” that returns an array containing image data (RGB value of each pixel in the image). Then, “find” function was used to recognize pixels for band by defining RGB values that are less than intensity of given bound (120 in the range of 0-255). Numbers of selected pixels were derived from this analysis.

Phosphopeptide immunoprecipitation

Phosphotyrosine (pY) peptides were purified using PhosphoScan pTyr100 (Cell Signaling) according to the manufacturer’s recommendations. Briefly, cells were treated with dasatinib (0.5 μM) or vehicle control (DMSO) for 3 hours in duplicate, and then whole cell extracts were prepared by denaturing lysis buffer containing 8 M urea, 20 mM HEPES (pH 8.0), supplemented with phosphatase inhibitors (1 mM sodium orthovanadate, 2.5 mM sodium pyrophosphate, and 1 mM β-glycerophosphate), followed by sonication on ice. Extracted proteins (75 mg each of control and dasatinib for H2286 cells and 70 mg each for HCC366 cells) were then reduced with 4.5 mM DTT and alkylated with 10 mM iodoacetamide. Trypsin digestion was carried out at room temperature overnight, and resulting tryptic peptides were then acidified with 1% trifluoroacetic acid and desalted with C18 Sep-Pak cartridges according to the manufacturer’s procedure. Peptides were lyophilized and then dissolved in immune-affinity purification (IAP) buffer containing 50 mM MOPS (pH 7.2), 10 mM sodium phosphate, and 50 mM sodium chloride. pY peptides were immunoprecipitated with immobilized pTyr-100 antibody (Cell Signaling) overnight at 4°C, followed by 3 washes with IAP buffer and 2 washes with H_2O. pY peptides were eluted from beads twice with 0.15% trifluoroacetic acid, and the volume was reduced to 20 μL via vacuum centrifugation. Before MS analysis, 100 fmol of horse myoglobin tryptic peptides were spiked in each sample to normalize quantification variation between MS runs. LC-MS/MS and statistical analysis of MS data are described in Supplementary Materials and Methods.

Generation of protein-protein interaction network for dasatinib-regulated pY proteins

pY proteins differentially regulated by dasatinib in both cell lines (n=73) were input into Cytoscape (version 2.8.3; http://cytoscape.org/) (17). Protein-protein interactions (PPIs) between nodes were then imported using BisoGenet plug-in (version 1.4; SysBiomics database) (18). The shapes of each node were determined by functional annotation via MetaCore (http://portal.genego.com) (19), and the direction of changes after dasatinib (upregulation, downregulation) was presented in unique color. The direction of change for proteins with multiple phosphopeptide data points was determined by majority voting.

Drug screening and synergy assessment

Viability assays were performed in 384-well microtiter plates in biological and technical duplicates. Viability was evaluated using the CellTiter-Glo assay (Promega), and luminescence was read on a SpectraMax M5 plate reader (Molecular Devices). Cells were seeded at a density of 1000 cells/well. Drugs were added after 24 hours, and cells were incubated for another 72 hours. For the synergy screen, dasatinib (at 0 μM and 0.1 μM, respectively) and each secondary drug (at 0.5 μM and 2.5 μM, respectively) were used. For determining three-dimensional dose-response surfaces, dasatinib concentrations ranged from 8 μM to 0.031 μM in 4-fold dilutions. Concentrations of all other drugs started at 10 μM and decreased in 4-fold increments to 0.039 μM. Drug combination effects were evaluated by the Bliss Model of Independence (20), setting the cut-off for depiction to 1 standard deviation. Independently, we applied the Chou-Talalay method using CompuSyn software (21). Combination index values for the replicates were averaged and corrected for the 95% confidence interval. The resulting corrected average combination index values were transformed to pCI values by generating the negative log in analogy to calculate pH values.

Mutational analysis of DDR2 in lung SCC tumor samples

Tumor tissues were collected as part of the Total Cancer Care™ protocol (22), and approved by the University of South Florida IRB. Patients gave informed written consent before enrollment in the Total Cancer Care protocol. Tumor tissues were snap frozen following lobectomy. All tissues contained more than 75% tumor cells examined by light microscopy. For DDR2 mutation analysis, tumor samples were subjected to genomic capture (performed by BGI, Shenzhen, China using SureSelect custom designs targeting 1,321 genes, Agilent Technologies, Inc., Santa Clara, CA) and massively parallel sequencing (performed by BGI, Shenzhen, China using GAIIx, Illumina, Inc., San Diego, CA). Sequences were aligned to the hs37d5 human reference with the Burrows-Wheeler Aligner (BWA) (23). Duplicate identification, insertion/deletion realignment, quality score recalibration, and variant identification were performed with PICARD (http://picard.sourceforge.net/) and the Genome Analysis ToolKit (GATK) (24). Sequence variants were annotated with ANNOVAR [PMC2938201] and visualized with mutationID, an in-house display tool. Potential protein-altering mutations were then identified in lung tumor samples. Those seen in the 1000 Genomes project were ignored as likely inherited germline variants. Sequence alignments were manually inspected with SAMtools tview (25) to remove artifact or low-quality mutations. Samples without any detectable DDR2 mutations were also identified for comparison studies.

Results

Characterization of phenotypic effects of dasatinib in DDR2-mutant lung cancer cell lines

We studied two DDR2-mutant lung SCC cell lines, the H2286 cell harboring a I638F mutation in the kinase domain and the HCC366 cell harboring a L239R mutation (7). We observed that dasatinib impaired viability of both DDR2-mutant cell lines in a dose-dependent manner (IC_{50} of 80.9 nM and 189.0 nM for H2286 and HCC366, respectively; Fig. 1A; see also Supplementary Fig. S1). However, maximum inhibition of cell viability was only between approximately 50% and 60% at physiologically relevant dasatinib

concentrations. We observed marginally increased apoptosis in H2286 (PARP cleavage), and cell cycle arrest and p27 induction were observed after dasatinib exposure in both cell lines (Fig. 1, B and C). Oncogenic driver RTKs in lung cancer (e.g., EGFR, EML4-ALK) promote cancer cell growth and survival via activation of two major downstream signaling pathways, RAF-MEK-ERK and PI3K-AKT (26, 27). In addition, because DDR2 stimulation by collagen I has been shown to lead to increased ERK phosphorylation in a breast cancer cell line (28), we tested whether dasatinib leads to decreased phosphorylation of ERK and AKT in H2286 and HCC366 cells. Dasatinib moderately reduced pAKT in H2286, but not in HCC366 cells. Notably, dasatinib failed to inhibit pERK in both DDR2-mutant cell lines to the same degree as observed with EGFR and ALK TKI in PC9 and H3122 cells, which harbor activating mutations in EGFR (exon 19 deletion) and ALK (EML4-ALK fusion), respectively (Fig. 1D). These results raised two possibilities: *1*) dasatinib inactivates downstream survival signals distinct from classic oncogenic RTKs and/or *2*) other RTKs compensate for the inhibition of dasatinib targets, thereby maintaining phosphorylation of ERK and AKT.

Phosphoproteomics reveals increased RTK activation following dasatinib exposure

As a multi-targeted kinase inhibitor, dasatinib is currently under clinical investigation in several human cancers, including lung cancer (12, 13, 29). We previously characterized comprehensive signaling pathways targeted by dasatinib in a panel of lung cancer cell lines lacking DDR2 mutations (8). Because signal transduction mediated by tyrosine phosphorylation plays a key role in cancer cell growth and survival, we characterized altered tyrosine phosphorylation after exposing DDR2-mutant lung SCC cells with dasatinib to gain further insight into dasatinib's action (30, 31). Our previous pharmacokinetic study in human lung cancer patients identified a C_{max} of dasatinib ranging from 100 to 300 ng/mL (204-615 nM) (12); thus 500 nM was chosen for phosphoproteomics experiments. H2286 and HCC366 cells were exposed to dasatinib (500 nM, 3 hours) or vehicle control (DMSO), and then tyrosine-phosphorylated peptides were purified by immunoaffinity capturing using anti-pY antibodies coupled with liquid chromatography and tandem mass spectrometry (LC-MS/MS) as performed in our previous studies (8, 16) (Fig. 2). From this approach, we identified a total of 543 and 636 unique pY peptides from H2286 and HCC366, respectively (Supplementary Table S1). As part of quality control (QC), pY peptides identified only in one or two replicates (out of total of 8 LC-MS/MS per cell line) were removed; thus pY peptides identified in at least three replicates were selected for further analysis. Next, the results from the 2-sample t-test for each pY peptides were used to identify differentially phosphorylated peptides after adjusting for multiple comparison using q-value of 20% (see Supplementary Materials and Methods), resulting in 207 pY peptides (corresponding to 173 pY proteins) and 259 pY peptides (corresponding to 195 pY proteins) from H2286 and HCC366, respectively (Supplementary Table S2). We named these pY peptides as "dasatinib-regulated pY peptides" and the corresponding pY proteins as "dasatinib-regulated pY proteins." We further filtered out dasatinib-regulated pY proteins identified only in one cell line, focusing on those identified in both cell lines (73 unique pY proteins; Supplementary Table S3). To gain an architectural view of dasatinib-regulated pY signaling in DDR2-mutant lung cancer cells, the resulting 73 pY proteins were mapped to the BisoGenet PPI network (18).

The PPI network revealed interaction hubs of reduced tyrosine phosphorylation of SFKs, including SRC and LYN, which were connected to their targets BCAR1 (also called p130 Cas), SHB, and NEDD9 (Fig. 3A) (8, 32, 33). This is consistent with our previous pY profiling, which showed that dasatinib led to decreased phosphorylation of SFKs and their targets (8). Interestingly, we were unable to detect tyrosine phosphorylated peptides corresponding to DDR2 in either of the two SCC cell lines studied, despite our ability to detect these peptides in previous studies of lung and sarcoma cell lines (8, 16). These results are consistent with recent studies showing low levels of tyrosine phosphorylation of I638F DDR2 mutations in engineered HEK293 cells (15). Unexpectedly, the network also centered increased tyrosine phosphorylated RTKs, including EGFR, IGF-1R, and ERBB2/HER2. We similarly observed increased tyrosine phosphorylation of Grb-associated Binder 1 (GAB1), insulin receptor substrate 2 (IRS2), and fibroblast growth receptor substrate 2 (FRS2), which are downstream adaptor proteins for a panel of various RTKs (34-36). Inspection of extracted ion chromatograms (EIC) for pY peptides was performed to verify these findings. While dasatinib reduced tyrosine phosphorylation of pY sites associated with SRC activity in EGFR (Y869) and ERBB2 (Y877) (37, 38), we observed dasatinib increased tyrosine phosphorylations required for kinase activity of oncogenic RTKs as well as increased tyrosine phosphorylation of downstream adaptor molecules (Fig. 3B and Table 1). We extended EIC analysis to other RTKs, including MET and AXL, and found that dasatinib increased EIC of pY peptides for these RTKs in both cell lines as well. For further validation, we performed targeted multiple reaction monitoring (MRM) for selected pY peptide 39) and verified that dasatinib leads to increased tyrosine phosphorylation of IGF-1R and EGFR (Supplementary Fig. S2). Together, our pY profiling revealed decreased tyrosine phosphorylation of predominantly SFK targets as well as provided evidence of secondary activation of RTKs following dasatinib exposure.

Small-molecule screening identifies RTK inhibitors that synergize with dasatinib

Recent studies have reported that ablation of key survival signaling molecules often activate secondary survival mechanisms that compensate for loss of survival signaling, further providing rationale for drug combination (40, 41). We thus systematically assessed drug combinations that could enhance dasatinib efficacy in lung cancer cells with DDR2 mutations. We screened 180 targeted small-molecule compounds in combination with dasatinib (0 or 0.1 μM) in H2286 and HCC366 cells and examined cell viability. Intriguingly, this specifically highlighted TKIs targeting RTKs whose tyrosine phosphorylation was enhanced by dasatinib identified through our mass spectrometry analysis: IGF-1R inhibitors (BMS-754807, GSK1838705A, linsitinib), EGFR/HER2 inhibitors (erlotinib, lapatinib), and MET/AXL inhibitors (crizotinib, cabozantinib). In H2286 cells, most of the above TKIs showed at least additive effects when combined with dasatinib (ratio >1), whereas some drug combination showed marginal effects in HCC366 cells (Fig. 4A, Supplementary Table S4). We therefore evaluated the observed positive drug cooperativity in more detail by generating three-dimensional dose-response matrices that are delineated by the individual single drugs. Target inhibition of these TKIs was validated by Western blotting (Supplementary Fig. S3). The subsequent analyses using the Bliss Model of Independence (20) indicated that MET/AXL and IGF-1R inhibitors in combination with dasatinib showed pronounced synergistic effects at most doses in both cell lines (with the

exception of dasatinib + crizotinib in HCC366), but also suggested some weak synergy between dasatinib and the EGFR/HER2 inhibitor lapatinib (Fig. 4, B and C, and Supplementary Table S5). Independent analysis using Combination Index (CI) method reported by Chou-Talalay (21) validated these assessments. Consistently, co-targeting IGF-1R or MET/AXL with dasatinib showed pronounced synergistic effects at most doses, whereas EGFR/HER2 TKI showed less positive cooperativity with dasatinib (Supplementary Fig. S4). We next tested if these combinations could lead to decreased oncogenic downstream signals of RTKs, pERK, and pAKT, as well as global tyrosine phosphorylation. In H2286 cells, co-targeting MET/AXL with dasatinib significantly reduced pERK, pAKT, and global tyrosine phosphorylation (pY100), and co-targeting IGF-1R showed the most pronounced reductions in HCC366 cells (Fig. 4, D and E). Notably, these results are correlated with the drug synergy analysis that showed that crizotinib (MET TKI) and BMS-754807 (IGF-1R TKI) were strongly synergistic with dasatinib in H2286 and HCC366, respectively (Fig. 4, B and C). Collectively, our drug screening showed that combined targeting of RTKs, especially IGF-1R and MET/AXL, could enhance the efficacy of dasatinib in DDR2-mutant lung SCC cells.

Growth factor-driven resistance to dasatinib

We described that dasatinib led to increased tyrosine phosphorylation in a panel of RTKs, including EGFR and MET, and that dual dasatinib and select RTK inhibitors were synergistic. These results indicate that survival signals induced by these RTKs could be redundant with those driven by dasatinib targets. It has been reported that RTK ligands confer drug resistance to kinase inhibitors in kinase-addicted cancer cells, raising the possibility of ligand-induced dasatinib resistance (42, 43). We thus tested whether the efficacy of dasatinib could be impaired by exogenous RTK ligands. We focused on RTKs whose tyrosine phosphorylation was enhanced upon dasatinib treatment (EGFR, MET, IGF-1R, and AXL). Cells were concomitantly treated with dasatinib in combination with EGF, HGF, IGF1, and GAS6, ligands for EGFR, MET, IGF-1R, and AXL, respectively. Among these RTK ligands, EGF showed the most pronounced rescue effect in both cell lines (Fig. 5, A and B). HGF rescued only HCC366, consistent with our observation that HGF failed to stimulate MET in H2286 (Supplementary Fig. S5). EGF impaired p27 induction after dasatinib exposure in both cell lines, as did HGF in HCC366, indicating that RTK stimulation relieved cell cycle arrest by dasatinib (Fig. 5C). We failed to observe any rescue effects of IGF1 and GAS6, despite their ability to induce receptor activation. Collectively, these data suggest that crosstalk between dasatinib targets and various other RTKs contribute to signaling for cancer cell survival; in addition, exogenous ligands could prime dasatinib resistance in DDR2-mutant lung cancer cells.

Evidence of intrinsic dasatinib-resistant mechanism by EGFR and MET in human lung SCC tissue

We next asked whether these RTKs that can drive dasatinib resistance exist in human lung cancer tissues harboring DDR2 mutations. Studies have shown that growth factors generated from the tumor microenvironment can support cancer cell survival, further inducing drug resistance by potentiating RTK activity in cancer cells (44-46). Cancer cells typically express multiple growth factor receptors (e.g., EGFR, MET); thus it is possible that stroma-

driven intrinsic RTK activities and mutational DDR2 could provide growth and survival signaling in a cooperative manner. To support this idea, we analyzed intrinsic RTK activity in lung SCC tumors via tyrosine phosphorylation of EGFR, MET, IGF-1R, and AXL in primary human lung SCC samples with defined DDR2 mutational status (n=4; Fig. 6A). Notably, two lung SCC tissues expressed high levels of both total and phospho-EGFR (tumor b and c), with one observed sample having high MET in total and phospho-level (tumor d; Fig. 6B). We could not observe clear evidence of IGF-1R and AXL phosphorylation in tumors tested. These data suggest that a subgroup of DDR2-mutant lung cancers expressing high levels of RTK activation could contribute to reduced efficacy of targeted therapy against DDR2.

Discussion

Our approach focusing on tyrosine phosphoproteomics was utilized to dissect oncogenic signaling through analyses of differentially regulated pY sites following dasatinib treatment in DDR2-mutant lung SCC cell lines. RTKs activate their downstream signals by forming a signaling complex composed of adaptor molecules, including GRB2, GAB1, SHC1 (for activation of MAPK signaling), and PI3K (for PI3K-AKT signaling). Our pY profiling however showed that tyrosine phosphorylation of SHC1 and PIK3 was not significantly affected by dasatinib, suggesting that dasatinib inhibits downstream signals through a mechanism distinct from classic oncogenic RTK inhibition. This is consistent with our data showing that dasatinib induced only a modest reduction in pERK in DDR2-mutant cells unlike other TKIs in EGFR and EML4-ALK systems (Fig. 1D). Instead, the majority of reduced tyrosine phosphorylation was associated with reduced activity of SFK and its downstream substrates.

The most notable finding from our study is that dasatinib led to increased tyrosine phosphorylation of a panel of RTKs (EGFR, MET, IGF-1R, AXL) and their downstream adaptors, including GAB1 and IRS2. This suggested the presence of RTK-driven adaptive resistance mechanisms following dasatinib. Growth factor RTK signaling is tightly regulated by negative-feedback pathways, which limit overstimulation of RTK itself or its downstream signaling molecules. Thus, targeting growth factor signaling blocks oncogenic signaling, but also relieves the negative-feedback mechanism, which leads to compensatory activation of parallel RTKs and adaptive drug resistance (47). Compensatory RTK activation has been repeatedly observed from our previous phosphoproteomics approaches. Profiling tyrosine phosphorylation of lung cancer cells using Src-homolog-2 (SH2) domains revealed evidence of increased tyrosine phosphorylation following EGFR TKI (48). Similarly, erlotinib (EGFR TKI) increased tyrosine phosphorylation of MET and IRS2 in *EGFR*-mutant cells (49). KRAS-mutant lung cancer cells adapt to knockdown of serine/threonine kinase TBK1 via increasing tyrosine phosphorylation of a panel of RTKs, including EGFR and MET (50). These findings suggest that the compensatory RTK activation attenuates kinase inhibitor efficacy, suggesting that co-targeting these adaptive RTKs could lead to synergistic effects. This notion was supported by results showing that dual targeting of these RTKs caused a synergistic effect with dasatinib and that ligand stimulation of RTKs decreased the efficacy of dasatinib. We also provided evidence of intrinsic RTK activity in primary human lung SCC samples with DDR2 mutations; 3 of 4

DDR2-mutant SCC tissues expressed high levels of tyrosine phosphorylated EGFR or MET. Our tumor tissue samples were not treated with dasatinib; thus the origin of RTK activity in the tumor samples is different from inducible RTK activation observed in our pY profiling. However, it is still noteworthy that a set of lung SCC tumors was shown to already harbor intrinsic RTK activity, since modulation of RTK activity affected the efficacy of dasatinib. It is possible that the intrinsic RTK activity in the tumors could be primed under certain conditions such as the presence of dasatinib combined with aberrant stromal activation, possibly leading to drug resistance. This is in accordance with our results showing that stimulation of EGFR by EGF rescued loss of cell viability by dasatinib.

The underlying mechanism whereby dasatinib leads to increased RTK activity in these DDR2-mutant cells remains unclear. Whereas previous studies have shown upregulation of RTK expression following targeted kinase inhibition (40, 41), this may not be the case for our results. The former studies showed transcriptional upregulation of RTKs following prolonged exposure of drugs (>24 hours), while we observed increased tyrosine phosphorylation in RTKs after 3 hours of dasatinib exposure. Dasatinib did not affect the total level of RTKs in this time frame; thus it appears that dasatinib turns on RTK activity via an unknown mechanism. Possibilities include increased ligand production by tumor cells (e.g., EGF, HGF) or decreased activity of tyrosine phosphatases targeting oncogenic RTKs as has been reported for PTPN12 (51). In our study, dasatinib significantly reduced tyrosine phosphorylation in a panel of tyrosine phosphatases, including PTPN6 (−4.26 fold at Y564 in HCC366 cells) and PTPN11 (−1.9 fold at Y62 in H2286 cells; Supplementary Table S2), providing a possibility of co-targeting of tyrosine phosphatases to suppress compensatory RTK activation.

A recent study analyzed global tyrosine phosphorylation changes after collagen stimulation, a well-established DDR2 ligand, in HEK293 cells ectopically expressing DDR2 (15). This study offered us an opportunity to identify overlap between select tyrosine phosphorylations specifically driven by DDR2 and decreased pY proteins following dasatinib treatment. One notable pY protein whose phosphorylation was increased after DDR2 stimulation (by collagen) and decreased by dasatinib was NCK1 (noncatalytic region of tyrosine kinase 1), an oncogenic adaptor molecule containing a C-terminal SH2 and three N-terminal SH3 domains (−5.38 fold at Y112 in H2286 cells; Supplementary Table S2). Like other SH2/SH3 domain-containing proteins, NCK1 associates with tyrosine phosphorylated growth factor RTKs via its SH2 domain, subsequently is tyrosine phosphorylated, and then bridges RTKs to proline-rich downstream effectors via the SH3 domain. Functionally diverse downstream effectors of NCK1 exist (52), including SOS GTP-exchange factor (GEF) for RAS activation (53), which suggests NCK1 potentially links DDR2 to MAPK signaling. Other NCK1 downstream molecules include p21-activated kinases (PAKs) and associated GTPase proteins such as Cdc42 and Rac1 (54, 55). These suggest DDR2 would be also linked to Rho family GTPase signal leading to cellular proliferation or cytoskeleton reorganization. Further investigation of NCK1 function in DDR2 survival signal (for example, via NCK1 knockdown experiments or mapping the physical PPI for DDR2 and NCK1) may provide further insight into DDR2 survival signaling.

Dasatinib has been approved for the treatment of chronic myeloid leukemia and Philadelphia chromosome-positive acute lymphoblastic leukemia. Due to its broad efficacy against multiple oncogenic kinases, including SFK and a panel of RTKs, clinical efficacy of dasatinib is currently being explored in several solid tumors, including NSCLC (12, 13, 29). Here, we revealed the potential RTK-driven adaptive resistant mechanisms for dasatinib in DDR2-mutant lung SCC cells through characterizing dasatinib-regulated global tyrosine phosphorylation. This indicates that co-targeting of compensatory RTKs could be beneficial, with our findings leading to better designed future clinical trials for SCC lung cancer harboring DDR2 mutations.

Supplementary Material

Refer to Web version on PubMed Central for supplementary material.

Acknowledgements

We thank Rasa Hamilton (Moffitt Cancer Center) for editorial assistance and Dr. Eunjung Kim (Moffitt Integrated Mathematical Oncology group) for her assistance with Western blotting quantification. This Total Cancer Care® study was enabled, in part, by the generous support of the DeBartolo Family, and we thank the many patients who so graciously provided data and tissue for this study. Our study also received valuable assistance from the Proteomics and Bioinformatics Core Facility at the H. Lee Moffitt Cancer Center & Research Institute, an NCI-designated Comprehensive Cancer Center, supported under NIH grant P30-CA76292.

Grant Support

This work was supported, in whole or in part, by National Institutes of Health SPORE Grant P50 CA119997.

References

1. Weir BA, Woo MS, Getz G, Perner S, Ding L, Beroukhim R, et al. Characterizing the cancer genome in lung adenocarcinoma. Nature. Dec 6; 2007 450(7171):893–8. [PubMed: 17982442]
2. Pao W, Iafrate AJ, Su Z. Genetically informed lung cancer medicine. J Pathol. Jan; 2011 223(2): 230–40. [PubMed: 21125677]
3. Weiss J, Sos ML, Seidel D, Peifer M, Zander T, Heuckmann JM, et al. Frequent and focal FGFR1 amplification associates with therapeutically tractable FGFR1 dependency in squamous cell lung cancer. Sci Transl Med. Dec 15.2010 2(62):62ra93.
4. Yamamoto H, Shigematsu H, Nomura M, Lockwood WW, Sato M, Okumura N, et al. PIK3CA mutations and copy number gains in human lung cancers. Cancer Res. Sep 1; 2008 68(17):6913–21. [PubMed: 18757405]
5. Comprehensive genomic characterization of squamous cell lung cancers. Nature. [Research Support, N.I.H., Extramural]. Sep 27; 2012 489(7417):519–25.
6. Vogel W. Discoidin domain receptors: structural relations and functional implications. FASEB J. 1999; 13(Suppl):S77–82. [PubMed: 10352148]
7. Hammerman PS, Sos ML, Ramos AH, Xu C, Dutt A, Zhou W, et al. Mutations in the DDR2 kinase gene identify a novel therapeutic target in squamous cell lung cancer. Cancer Discov. Jun; 2011 1(1):78–89. [PubMed: 22328973]
8. Li J, Rix U, Fang B, Bai Y, Edwards A, Colinge J, et al. A chemical and phosphoproteomic characterization of dasatinib action in lung cancer. Nat Chem Biol. Apr; 2010 6(4):291–9. [PubMed: 20190765]
9. Day E, Waters B, Spiegel K, Alnadaf T, Manley PW, Buchdunger E, et al. Inhibition of collagen-induced discoidin domain receptor 1 and 2 activation by imatinib, nilotinib and dasatinib. Eur J Pharmacol. Dec 3; 2008 599(1-3):44–53. [PubMed: 18938156]

10. Anastassiadis T, Deacon SW, Devarajan K, Ma H, Peterson JR. Comprehensive assay of kinase catalytic activity reveals features of kinase inhibitor selectivity. Nat Biotechnol. Nov; 2011 29(11): 1039–45. [PubMed: 22037377]
11. Davis MI, Hunt JP, Herrgard S, Ciceri P, Wodicka LM, Pallares G, et al. Comprehensive analysis of kinase inhibitor selectivity. Nat Biotechnol. Nov; 2011 29(11):1046–51. [PubMed: 22037378]
12. Haura EB, Tanvetyanon T, Chiappori A, Williams C, Simon G, Antonia S, et al. Phase I/II study of the Src inhibitor dasatinib in combination with erlotinib in advanced non-small-cell lung cancer. J Clin Oncol. Mar 10; 2010 28(8):1387–94. [PubMed: 20142592]
13. Johnson FM, Bekele BN, Feng L, Wistuba I, Tang XM, Tran HT, et al. Phase II study of dasatinib in patients with advanced non-small-cell lung cancer. J Clin Oncol. Oct 20; 2010 28(30):4609–15. [PubMed: 20855820]
14. Pitini V, Arrigo C, Di Mirto C, Mondello P, Altavilla G. Response to dasatinib in a patient with SQCC of the lung harboring a discoid-receptor-2 and synchronous chronic myelogenous leukemia. Lung Cancer. Oct; 2013 82(1):171–2. [PubMed: 23932362]
15. Iwai LK, Payne LS, Luczynski MT, Chang F, Xu H, Clinton RW, et al. Phosphoproteomics of collagen receptor networks reveals SHP-2 phosphorylation downstream of wild-type DDR2 and its lung cancer mutants. The Biochemical journal. Sep 15; 2013 454(3):501–13. [PubMed: 23822953]
16. Bai Y, Li J, Fang B, Edwards A, Zhang G, Bui M, et al. Phosphoproteomics identifies driver tyrosine kinases in sarcoma cell lines and tumors. Cancer Res. May 15; 2012 72(10):2501–11. [PubMed: 22461510]
17. Cline MS, Smoot M, Cerami E, Kuchinsky A, Landys N, Workman C, et al. Integration of biological networks and gene expression data using Cytoscape. Nat Protoc. 2007; 2(10):2366–82. [PubMed: 17947979]
18. Martin A, Ochagavia ME, Rabasa LC, Miranda J, Fernandez-de-Cossio J, Bringas R. BisoGenet: a new tool for gene network building, visualization and analysis. BMC Bioinformatics. 2010; 11:91. [PubMed: 20163717]
19. Ekins S, Nikolsky Y, Bugrim A, Kirillov E, Nikolskaya T. Pathway mapping tools for analysis of high content data. Methods Mol Biol. 2007; 356:319–50. [PubMed: 16988414]
20. Cokol M, Chua HN, Tasan M, Mutlu B, Weinstein ZB, Suzuki Y, et al. Systematic exploration of synergistic drug pairs. Molecular systems biology. 2011; 7:544. [PubMed: 22068327]
21. Chou TC. Drug combination studies and their synergy quantification using the Chou-Talalay method. Cancer Res. Jan 15; 2010 70(2):440–6. [PubMed: 20068163]
22. Fenstermacher DA, Wenham RM, Rollison DE, Dalton WS. Implementing personalized medicine in a cancer center. Cancer J. Nov-Dec;2011 17(6):528–36. [PubMed: 22157297]
23. Li H, Durbin R. Fast and accurate short read alignment with Burrows-Wheeler transform. Bioinformatics. Jul 15; 2009 25(14):1754–60. [PubMed: 19451168]
24. DePristo MA, Banks E, Poplin R, Garimella KV, Maguire JR, Hartl C, et al. A framework for variation discovery and genotyping using next-generation DNA sequencing data. Nat Genet. May; 2011 43(5):491–8. [PubMed: 21478889]
25. Li H, Handsaker B, Wysoker A, Fennell T, Ruan J, Homer N, et al. The Sequence Alignment/Map format and SAMtools. Bioinformatics. Aug 15; 2009 25(16):2078–9. [PubMed: 19505943]
26. Paez JG, Janne PA, Lee JC, Tracy S, Greulich H, Gabriel S, et al. EGFR mutations in lung cancer: correlation with clinical response to gefitinib therapy. Science. Jun 4; 2004 304(5676):1497–500. [PubMed: 15118125]
27. Koivunen JP, Mermel C, Zejnullahu K, Murphy C, Lifshits E, Holmes AJ, et al. EML4-ALK fusion gene and efficacy of an ALK kinase inhibitor in lung cancer. Clin Cancer Res. Jul 1; 2008 14(13):4275–83. [PubMed: 18594010]
28. Zhang K, Corsa CA, Ponik SM, Prior JL, Piwnica-Worms D, Eliceiri KW, et al. The collagen receptor discoidin domain receptor 2 stabilizes SNAIL1 to facilitate breast cancer metastasis. Nat Cell Biol. Jun; 2013 15(6):677–87. [PubMed: 23644467]
29. Kim LC, Rix U, Haura EB. Dasatinib in solid tumors. Expert Opin Investig Drugs. Mar; 2010 19(3):415–25.
30. Blume-Jensen P, Hunter T. Oncogenic kinase signalling. Nature. May 17; 2001 411(6835):355–65. [PubMed: 11357143]

31. Schlessinger J. Cell signaling by receptor tyrosine kinases. Cell. Oct 13; 2000 103(2):211–25. [PubMed: 11057895]
32. Karlsson T, Songyang Z, Landgren E, Lavergne C, Di Fiore PP, Anafi M, et al. Molecular interactions of the Src homology 2 domain protein Shb with phosphotyrosine residues, tyrosine kinase receptors and Src homology 3 domain proteins. Oncogene. Apr 20; 1995 10(8):1475–83. [PubMed: 7537362]
33. Ruest PJ, Shin NY, Polte TR, Zhang X, Hanks SK. Mechanisms of CAS substrate domain tyrosine phosphorylation by FAK and Src. Mol Cell Biol. Nov; 2001 21(22):7641–52. [PubMed: 11604500]
34. Haura EB, Smith MA. Signaling Control by Epidermal Growth Factor Receptor and MET: Rationale for Cotargeting Strategies in Lung Cancer. J Clin Oncol. Nov 10; 2013 31(32):4148–50. [PubMed: 24101046]
35. Kouhara H, Hadari YR, Spivak-Kroizman T, Schilling J, Bar-Sagi D, Lax I, et al. A lipid-anchored Grb2-binding protein that links FGF-receptor activation to the Ras/MAPK signaling pathway. Cell. May 30; 1997 89(5):693–702. [PubMed: 9182757]
36. Sawka-Verhelle D, Tartare-Deckert S, White MF, Van Obberghen E. Insulin receptor substrate-2 binds to the insulin receptor through its phosphotyrosine-binding domain and through a newly identified domain comprising amino acids 591-786. J Biol Chem. Mar 15; 1996 271(11):5980–3. [PubMed: 8626379]
37. Biscardi JS, Maa MC, Tice DA, Cox ME, Leu TH, Parsons SJ. c-Src-mediated phosphorylation of the epidermal growth factor receptor on Tyr845 and Tyr1101 is associated with modulation of receptor function. J Biol Chem. Mar 19; 1999 274(12):8335–43. [PubMed: 10075741]
38. Marcotte R, Zhou L, Kim H, Roskelly CD, Muller WJ. c-Src associates with ErbB2 through an interaction between catalytic domains and confers enhanced transforming potential. Mol Cell Biol. Nov; 2009 29(21):5858–71. [PubMed: 19704002]
39. Zhang G, Fang B, Liu RZ, Lin H, Kinose F, Bai Y, et al. Mass spectrometry mapping of epidermal growth factor receptor phosphorylation related to oncogenic mutations and tyrosine kinase inhibitor sensitivity. Journal of proteome research. Jan 7; 2011 10(1):305–19. [PubMed: 21080693]
40. Chandarlapaty S, Sawai A, Scaltriti M, Rodrik-Outmezguine V, Grbovic-Huezo O, Serra V, et al. AKT inhibition relieves feedback suppression of receptor tyrosine kinase expression and activity. Cancer cell. Jan 18; 2011 19(1):58–71. [PubMed: 21215704]
41. Duncan JS, Whittle MC, Nakamura K, Abell AN, Midland AA, Zawistowski JS, et al. Dynamic reprogramming of the kinome in response to targeted MEK inhibition in triple-negative breast cancer. Cell. Apr 13; 2012 149(2):307–21. [PubMed: 22500798]
42. Harbinski F, Craig VJ, Sanghavi S, Jeffery D, Liu L, Sheppard KA, et al. Rescue screens with secreted proteins reveal compensatory potential of receptor tyrosine kinases in driving cancer growth. Cancer Discov. Oct; 2012 2(10):948–59. [PubMed: 22874768]
43. Wilson TR, Fridlyand J, Yan Y, Penuel E, Burton L, Chan E, et al. Widespread potential for growth-factor-driven resistance to anticancer kinase inhibitors. Nature. Jul 26; 2012 487(7408): 505–9. [PubMed: 22763448]
44. Wang W, Li Q, Yamada T, Matsumoto K, Matsumoto I, Oda M, et al. Crosstalk to stromal fibroblasts induces resistance of lung cancer to epidermal growth factor receptor tyrosine kinase inhibitors. Clin Cancer Res. Nov 1; 2009 15(21):6630–8. [PubMed: 19843665]
45. Mink SR, Vashistha S, Zhang W, Hodge A, Agus DB, Jain A. Cancer-associated fibroblasts derived from EGFR-TKI-resistant tumors reverse EGFR pathway inhibition by EGFR-TKIs. Mol Cancer Res. Jun; 2010 8(6):809–20. [PubMed: 20530582]
46. Straussman R, Morikawa T, Shee K, Barzily-Rokni M, Qian ZR, Du J, et al. Tumour micro-environment elicits innate resistance to RAF inhibitors through HGF secretion. Nature. [Research Support, N.I.H., Extramural Research Support, Non-U.S. Gov't]. Jul 26; 2012 487(7408):500–4.
47. Chandarlapaty S. Negative feedback and adaptive resistance to the targeted therapy of cancer. Cancer Discov. Apr; 2012 2(4):311–9. [PubMed: 22576208]

48. Machida K, Eschrich S, Li J, Bai Y, Koomen J, Mayer BJ, et al. Characterizing tyrosine phosphorylation signaling in lung cancer using SH2 profiling. PloS one. 2010; 5(10):e13470. [PubMed: 20976048]

49. Yoshida T, Zhang G, Smith MA, Lopez AS, Bai Y, Li J, et al. Tyrosine Phosphoproteomics Identifies Both Codrivers and Cotargeting Strategies for T790M-Related EGFR-TKI Resistance in Non-Small Cell Lung Cancer. Clin Cancer Res. Jun 11.2014

50. Kim JY, Welsh EA, Oguz U, Fang B, Bai Y, Kinose F, et al. Dissection of TBK1 signaling via phosphoproteomics in lung cancer cells. Proc Natl Acad Sci U S A. Jul 23; 2013 110(30):12414–9. [PubMed: 23836654]

51. Sun T, Aceto N, Meerbrey KL, Kessler JD, Zhou C, Migliaccio I, et al. Activation of multiple proto-oncogenic tyrosine kinases in breast cancer via loss of the PTPN12 phosphatase. Cell. Mar 4; 2011 144(5):703–18. [PubMed: 21376233]

52. McCarty JH. The Nck SH2/SH3 adaptor protein: a regulator of multiple intracellular signal transduction events. BioEssays: news and reviews in molecular, cellular and developmental biology. Nov; 1998 20(11):913–21.

53. Hu Q, Milfay D, Williams LT. Binding of NCK to SOS and activation of ras-dependent gene expression. Mol Cell Biol. Mar; 1995 15(3):1169–74. [PubMed: 7862111]

54. Lu W, Katz S, Gupta R, Mayer BJ. Activation of Pak by membrane localization mediated by an SH3 domain from the adaptor protein Nck. Curr Biol. Feb 1; 1997 7(2):85–94. [PubMed: 9024622]

55. Galisteo ML, Chernoff J, Su YC, Skolnik EY, Schlessinger J. The adaptor protein Nck links receptor tyrosine kinases with the serine-threonine kinase Pak1. J Biol Chem. Aug 30; 1996 271(35):20997–1000. [PubMed: 8798379]

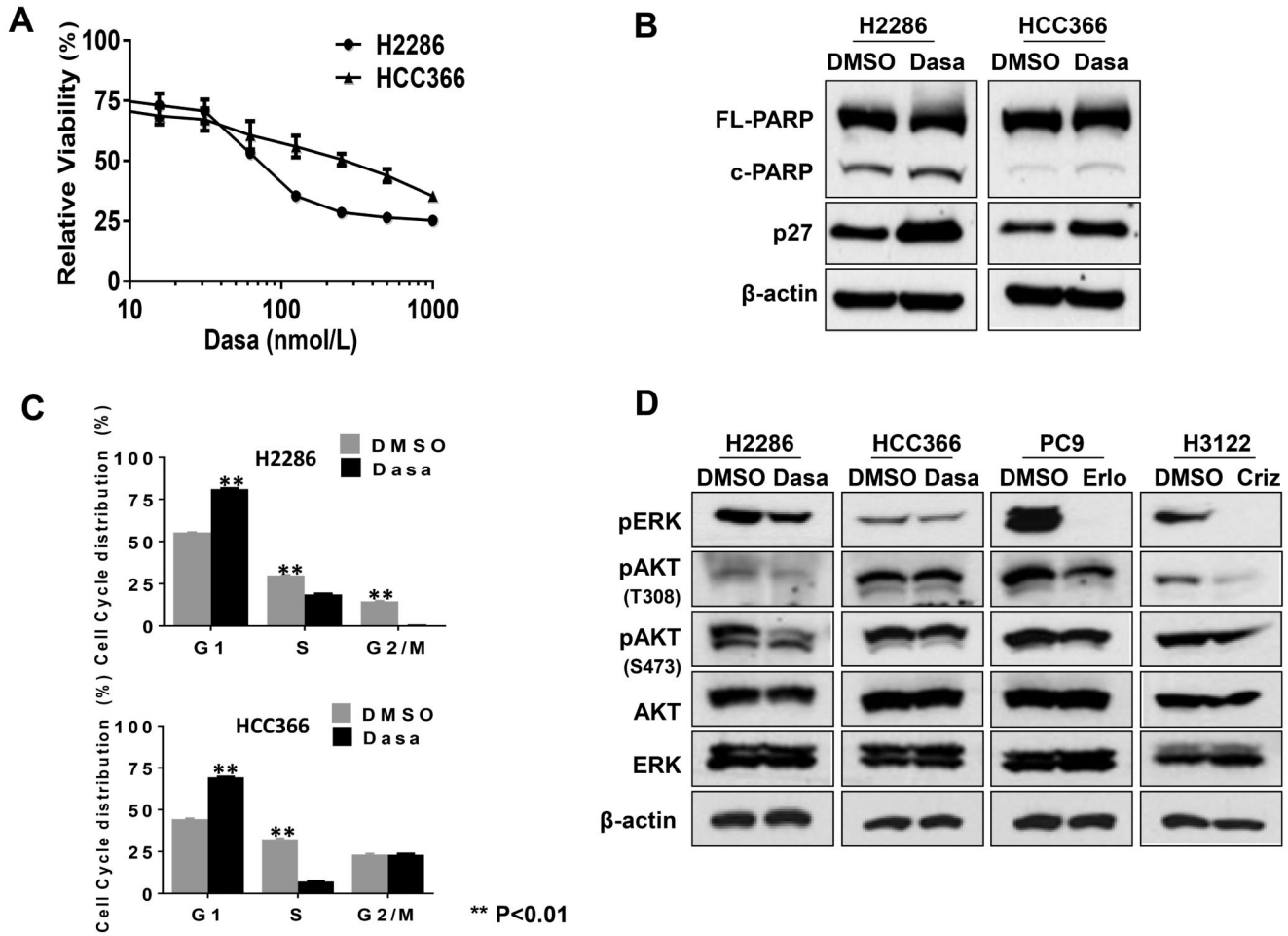

Fig. 1. Phenotypic effect of dasatinib (Dasa) on DDR2-mutant lung SCC cell lines, H2286 and HCC366

A: Relative cell viability after dasatinib treatment. Cells were treated with dasatinib for 96 hours, followed by cell viability assessed by CellTiter-Glo assay (Promega). Representative triplicates ± SD are presented, which showed similar results at least 3 times. **B:** p27 expression and PARP cleavage after dasatinib treatment (0.5 μM, 24 hours). **C:** Cell cycle profiling after dasatinib treatment (0.5 μM, 24 hours). **D:** Phosphorylation of ERK and AKT after tyrosine kinase inhibitor (TKI) treatment (0.5 μM, 3 hours). Erlo: erlotinib (EGFR TKI); Criz: crizotinib (ALK TKI). Intensity of each Western blot band was quantified and relative band intensity is shown in Fig. S1.

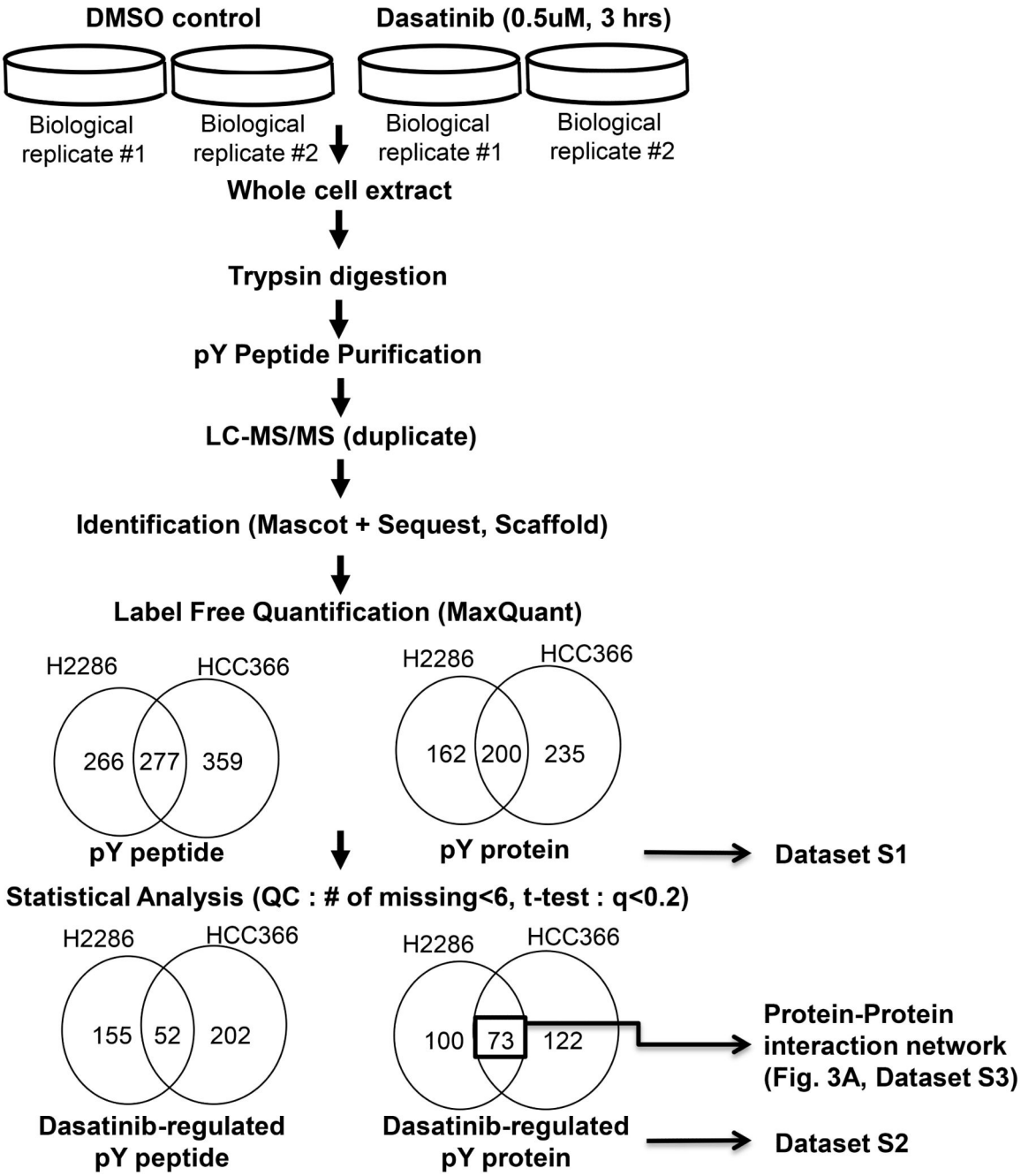

Fig. 2. Schematic of pY proteomics approach

Two DDR2-mutant lung SCC cell lines (H2286 and HCC366) were treated with dasatinib (500 μM, 3 hours) or DMSO vehicle control, followed by differential in pY peptides abundance analyzed by LC-MS/MS. Detailed methods for mass spectrometry and statistical analysis are described in Supplementary Materials and Methods.

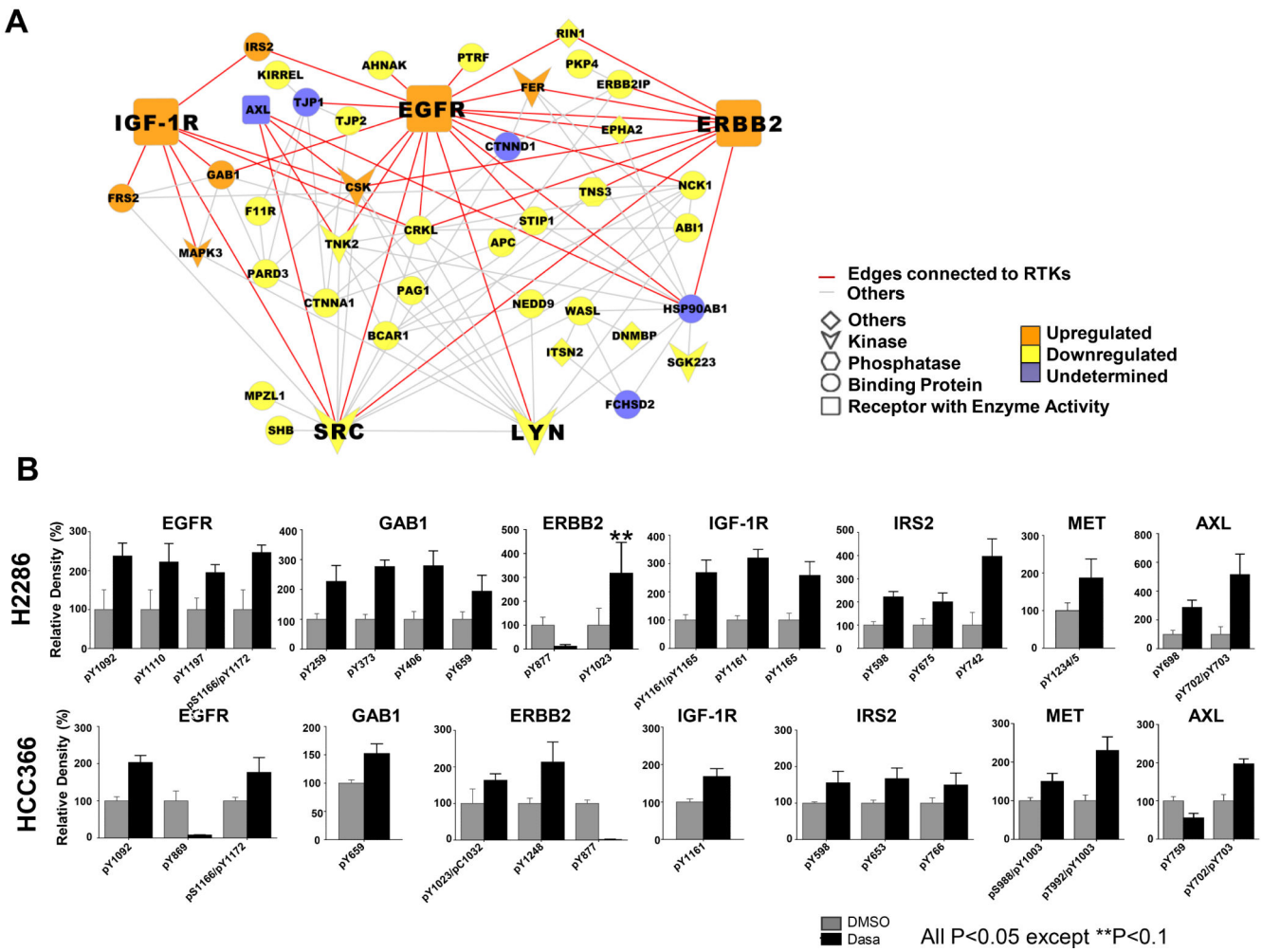

Fig. 3. Increased tyrosine phosphorylations in receptor tyrosine kinase (RTK) after dasatinib exposure

A: Protein-protein interaction (PPI) network composed of dasatinib-regulated pY proteins identified from both H2286 and HCC366 cells. Each protein was annotated based on its functional classification, with PPI then mapped utilizing BisoGenet Cytoscape plug-in. Increased tyrosine phosphorylation of EGFR, IGF-1R, and ERBB2 and decreased tyrosine phosphorylation of SRC and LYN are presented in bigger nodes. Edges connected to EGFR, IGF-1R and ERBB2 are shown in red, with others in gray. “Undetermined” signifies pY peptides showing conflicting direction (increased versus decreased) in the two cell lines. **B:** Extracted ion chromatogram (EIC) for pY peptides corresponding to RTK. Two-sample t-test was performed to address significant difference in EIC between control and dasatinib treatment.

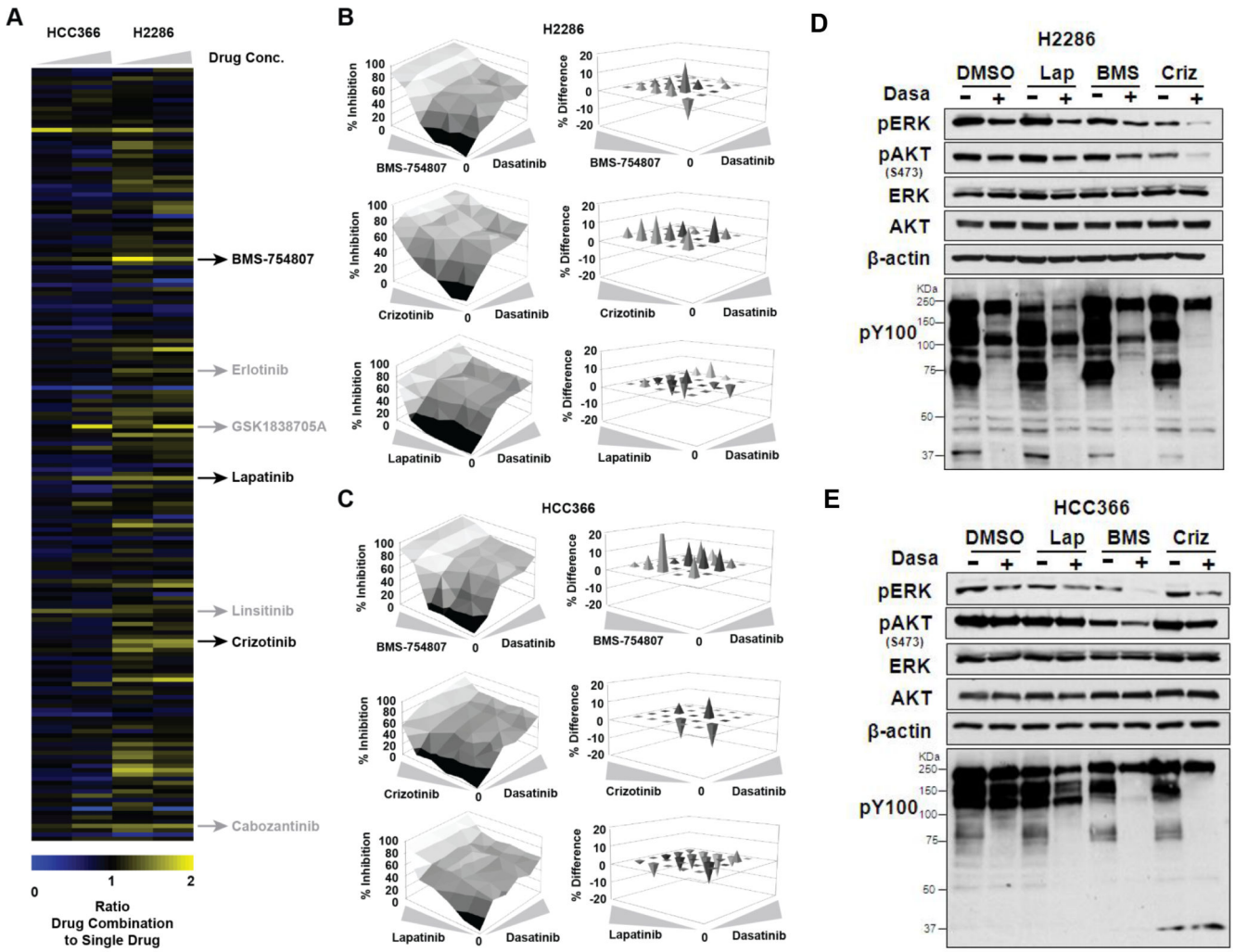

Fig. 4. Dasatinib-based drug combinations in DDR2-mutant lung SCC cells

A: Heat map depicting ratio of inhibition of cellular viability for HCC366 and H2286 cell lines by treatment with drug combinations (with 0.1 μM dasatinib) compared to single drug (no dasatinib) using a customized library of 180 targeted compounds. These compounds were tested at 0.5 μM and 2.5 μM as indicated by the drug concentration wedge. Drug combination results were normalized to effects elicited by 0.1 μM dasatinib alone. Indicated are dasatinib combinations with the IGF-1R/IR inhibitors BMS-754807, GSK1838705A, and linsitinib, with the MET/AXL inhibitors crizotinib and cabozantinib and with the EGFR inhibitors erlotinib and lapatinib (also inhibiting ERBB2). For a summary of Bliss analysis data, based on 6-by-6 point dose-response matrices, with these drug combinations, see Supplementary Table S5. **B** and **C:** Three-dimensional dose-response matrices delimited by individual single-drug dose-response curves displaying combination effects on viability of H2286 (**B**) and HCC366 (**C**) cells at various drug concentrations. Dasatinib concentrations ranged from 8 μM to 0.031 μM in 4-fold increments. Concentrations of BMS-754807, crizotinib, and lapatinib started at 10 μM and decreased in 4-fold increments to 0.039 μM. Needle graphs display the observed average difference in cell viability from additive drug

effects based on expected values that are calculated with the Bliss Model of Independence. Positive values indicate synergy, “0” denotes additivity, and negative values indicate antagonism. Only values greater than 1 standard deviation were considered significant and are depicted. **D** and **E:** Phosphorylation of ERK, AKT, and phosphotyrosine (pY100) after TKI treatment alone and in combination (0.5 μM for dasatinib, 1 μM for others, 3 hours) in H2286 (**D**) and HCC366 (**E**) cells. Lap: lapatinib (EGFR/HER2 TKI); BMS: BMS-754607 (IGF-1R TKI); Criz: crizotinib (MET/AXL TKI). Intensity of each Western blot band was quantified, and relative band intensity is shown in Fig. S1.

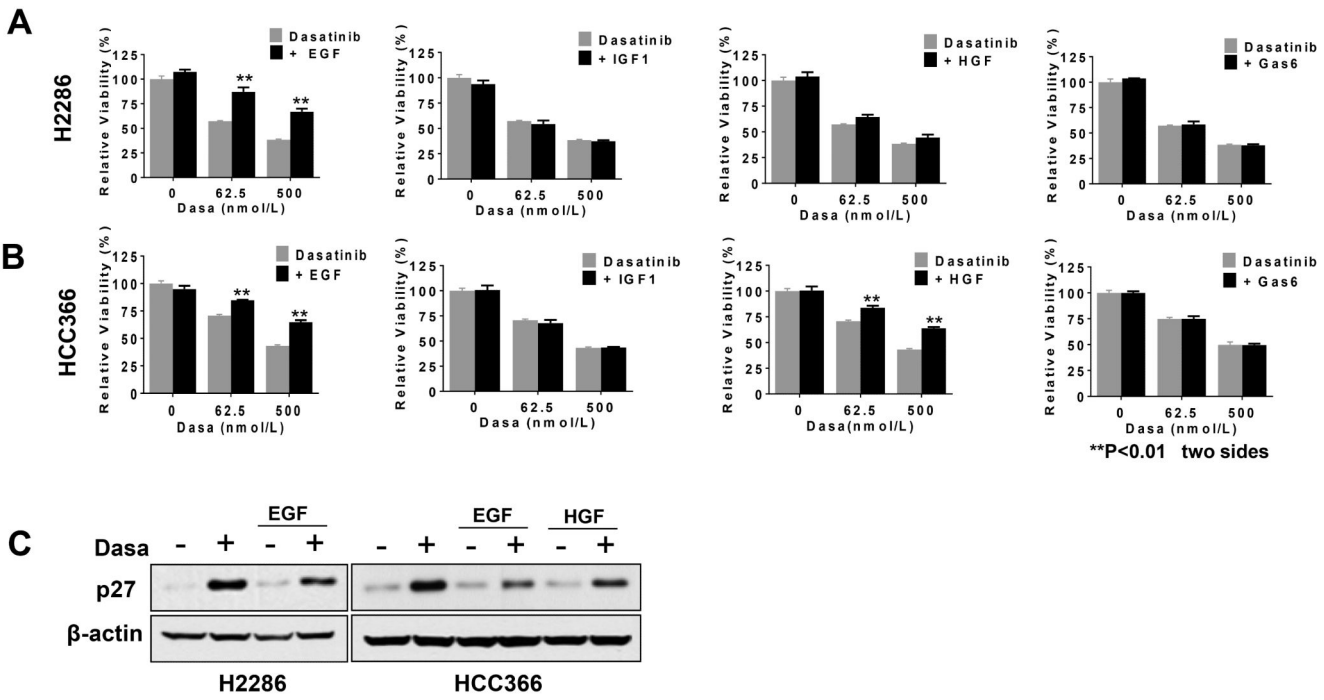

Fig. 5. Ligands for RTKs attenuate dasatinib efficacy

A and B: Effect of RTK ligands in dasatinib-mediated cell viability reduction. H2286 (**A**) and HCC366 (**B**) cells were concomitantly treated with dasatinib and indicated ligands (50 ng/mL for EGF, IGF1, and HGF and 800 ng/mL for GAS6) and then incubated for 72 hours before cell viability assay. Representative triplicates ± SD are presented, which showed similar results at least 3 times. **C:** p27 expression after dasatinib only or dasatinib (0.5 μM) in combination with RTK ligands (50 ng/mL). Whole cell extracts were prepared 24 hours after treatment.

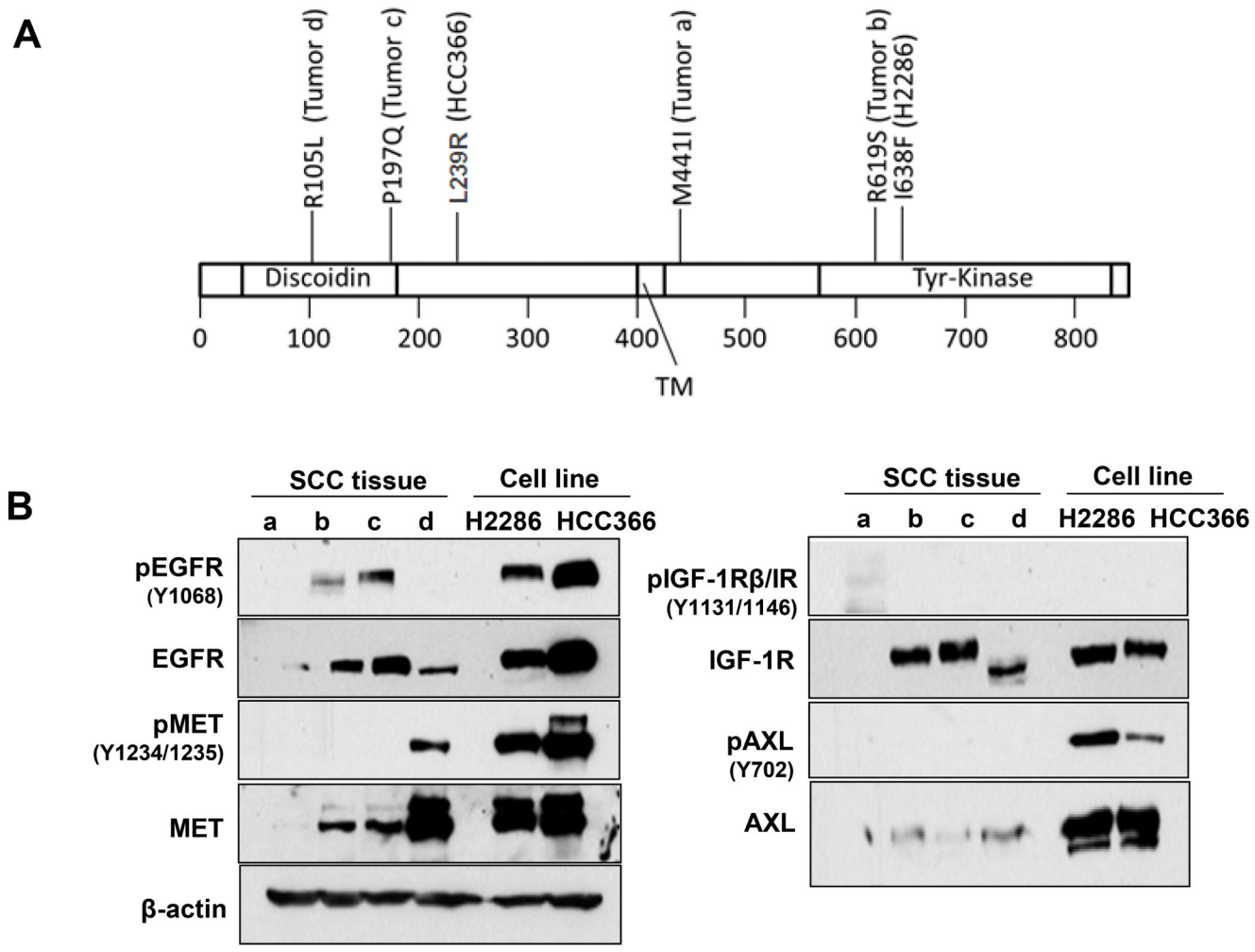

Fig. 6. RTK activation in human lung SCC tissues harboring DDR2 mutations

A: DDR2 missense mutations in primary lung SCC samples. Mutational status of H2286 and HCC366 cells are also indicated. TM, transmembrane. **B:** Whole cell extracts were prepared from 4 tumor samples or the 2 cell lines with DDR2 mutations and then subjected to Western blotting for phospho- and total RTK antibodies.

Table 1

Receptor tyrosine kinases and downstream adaptor molecules identified from phosphoproteomics

	pY site	Sequence	Autocatalysis site (Y/N)	Fold Change	*P* value
H2286					
EGFR	pY1092	YSSDPTGALTEDSIDDTFLPVPEyINQSVPK	Y	2.37	0.0352
	pS1166/pY1172	GSHQIsLDNPDyQQDFFPK	N/Y	2.46	0.0148
	pY1110	RPAGSVQNPVyHNQPLNPAPSR	Y	2.22	0.0007
	pY1197	GSTAENAEyLR	Y	1.95	0.0272
GAB1	pY259	APSASVDSSLyNLPR		2.27	0.04
	pY373	TASDTDSSyCIPTAGMSPSR		2.76	0.00
	pY406	DASSQDCyDIPR		2.80	0.01
	pY659	SSGSGSSVADERVDyVVVDQQK		1.94	0.01
ERBB2	pY1023	SLLEDDDMGDLVDAEEyLVPQQGFFCPDPAPGAGGMVHHR	N	3.18	0.0803
	pY877	LLDIDETEyHADGGKVPIK	N	−8.20	0.0155
IGF-1R	pY1161/pY1165	DIyETDyYRK	Y/N	2.68	0.0016
	pY1161	DIyETDYYR	Y	3.20	0.0012
	pY1165	DIYETDyYR	N	2.58	0.0017
IRS2	pY598	QRPVPQPSSASLDEyTLMR		2.22	0.0035
	pY675	SDDyMPMSPASVSAPK		2.00	0.0096
	pY742	ASSPAESSPEDSGyMR		3.97	0.0112
MET	pY1234/5	DMYDKEyySVHNK	Y/Y	1.87	0.0419
AXL	pY698	KIyNGDYYR	N	2.87	0.0046
HCC366					
EGFR	pY1092	YSSDPTGALTEDSIDDTFLPVPEyINQSVPK	Y	2.03	0.0003
	pS1166/pY1172	GSHQIsLDNPDyQQDFFPK	N/Y	1.77	0.0165
	pY869	LLGAEEKEyHAEGGKVPIK	N	−11.91	0.0066
GAB1	pY659	SSGSGSSVADERVDyVVVDQQK		1.52	0.0159
ERBB2	pY1023	SLLEDDDMGDLVDAEEyLVPQQGFFCPDPAPGAGGMVHHR	N	1.63	0.0224
	pY1248	GAPPSTFKGTPTAENPEyLGLDVPV	Y	2.13	0.0128
	pY877	LLDIDETEyHADGGKVPIK	N	−63.28	0.0002
IGF-1R	pY1161	DIyETDYYRK	Y	1.68	0.0166
IRS2	pY598	QRPVPQPSSASLDEyTLMR		1.56	0.0404
	pY653	SSSSNLGADDGyMPMTPGA		1.67	0.0078
	pY766	LLPNGDyLNVSPSDAVTTG		1.50	0.0478
	pY978	SPLSDyMNLDFSSPK		1.56	0.0317
MET	pS988/pY1003	sVSPTTEMVSNESVDyR	N/N	1.50	0.0141
	pT992/pY1003	SVSPtTEMVSNESVDyR	N/N	2.30	0.0020
AXL	pY702/pY703	IYNGDyyRQGR	N/Y	1.97	0.0039
	pY759	GQTPYPGVENSEIyDYLR	N	−1.79	0.0001

Fold change indicates the intensity of extracted ion chromatogram (EIC) after dasatinib treatment. Phosphorylated amino acids are shown in lowercase letters.